Supplementary Figure 1

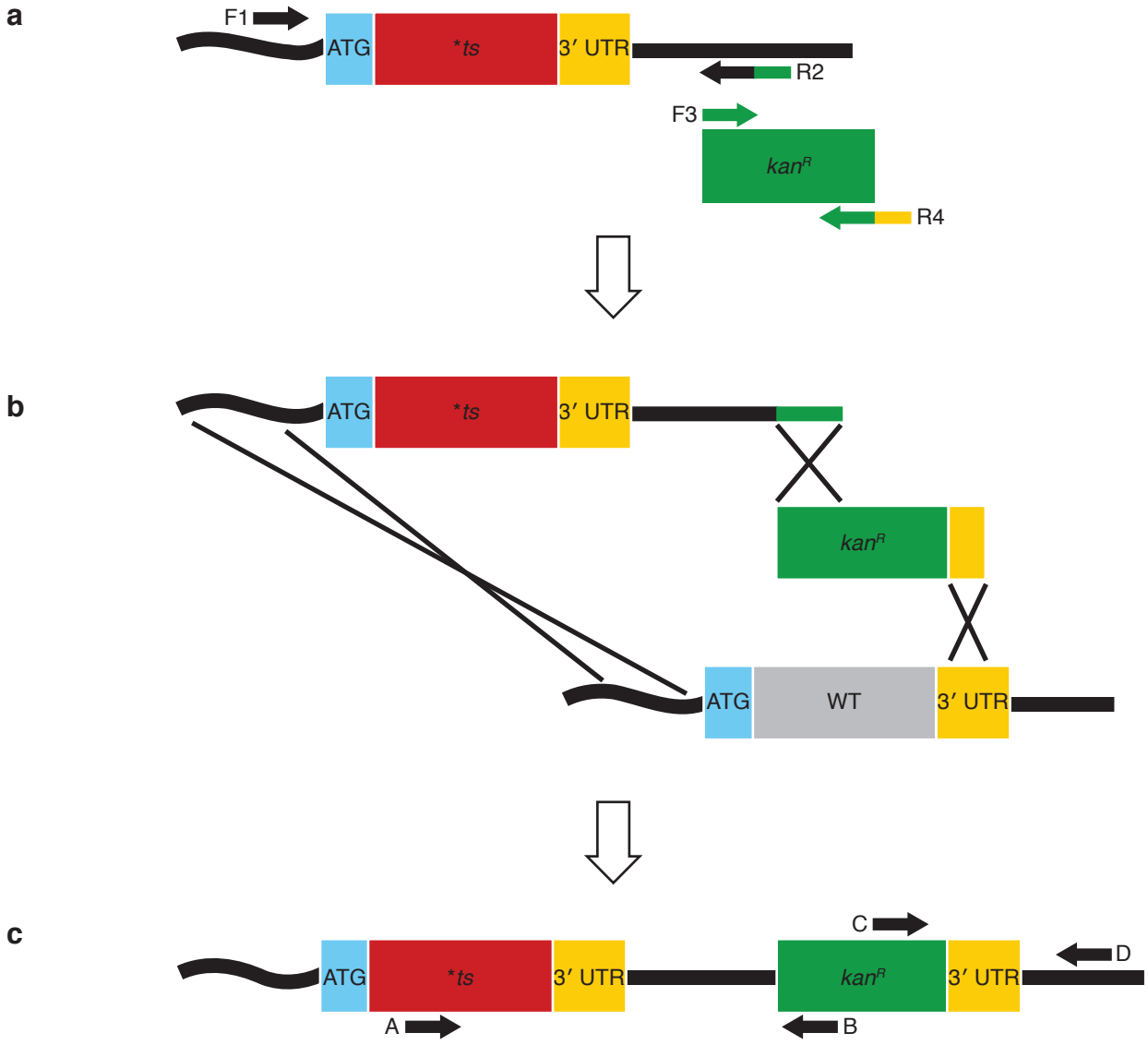

Supplementary Figure 1. Construction of Temperature-sensitive Strains
(a) Strategy for constructing strains harboring ts alleles of essential genes is depicted (not drawn to scale). A ts allele including 200-350 bp downstream of its stop codon was amplified by PCR using primers F1 and R2. The *kanMX* cassette was amplified by PCR using primers F3 and R4. The F1 primer sequence is unique to a region 50-400 bp upstream of the ts allele ATG while the R2 primer sequence is complementary to a region 200-350 bp downstream of the stop codon and includes an additional 32 to 36 bp sequence complementary to the 5' end of the TEF promoter. The F3 primer sequence is unique to the TEF promoter and primer R4 sequence is complementary to the TEF terminator of the *kanMX* cassette and a 45 bp sequence immediately downstream of the ts allele stop codon. The F3 primer sequence is AGATCTGTTTAGCTTGCCTCGTCC and sequences for F1, R2, and R4 primers are listed in **Supplementary Table 2**. **(b)** The wild-type ORF was replaced by *ts allele::kanMX* through homologous recombination. **(c)** Two PCR reactions were used to confirm proper integration of the ts allele and *kanMX* cassettes. Primers A and B diagnosed linkage of *kanMX* cassette to the target gene. Primers C and D verified integration of the ts allele::kanMX at the target gene locus. The primer sequences for confirmation PCR are listed in **Supplementary Table 2**.

Nature Biotechnology: doi:10.1038/nbt.1832

Supplementary Figure 2

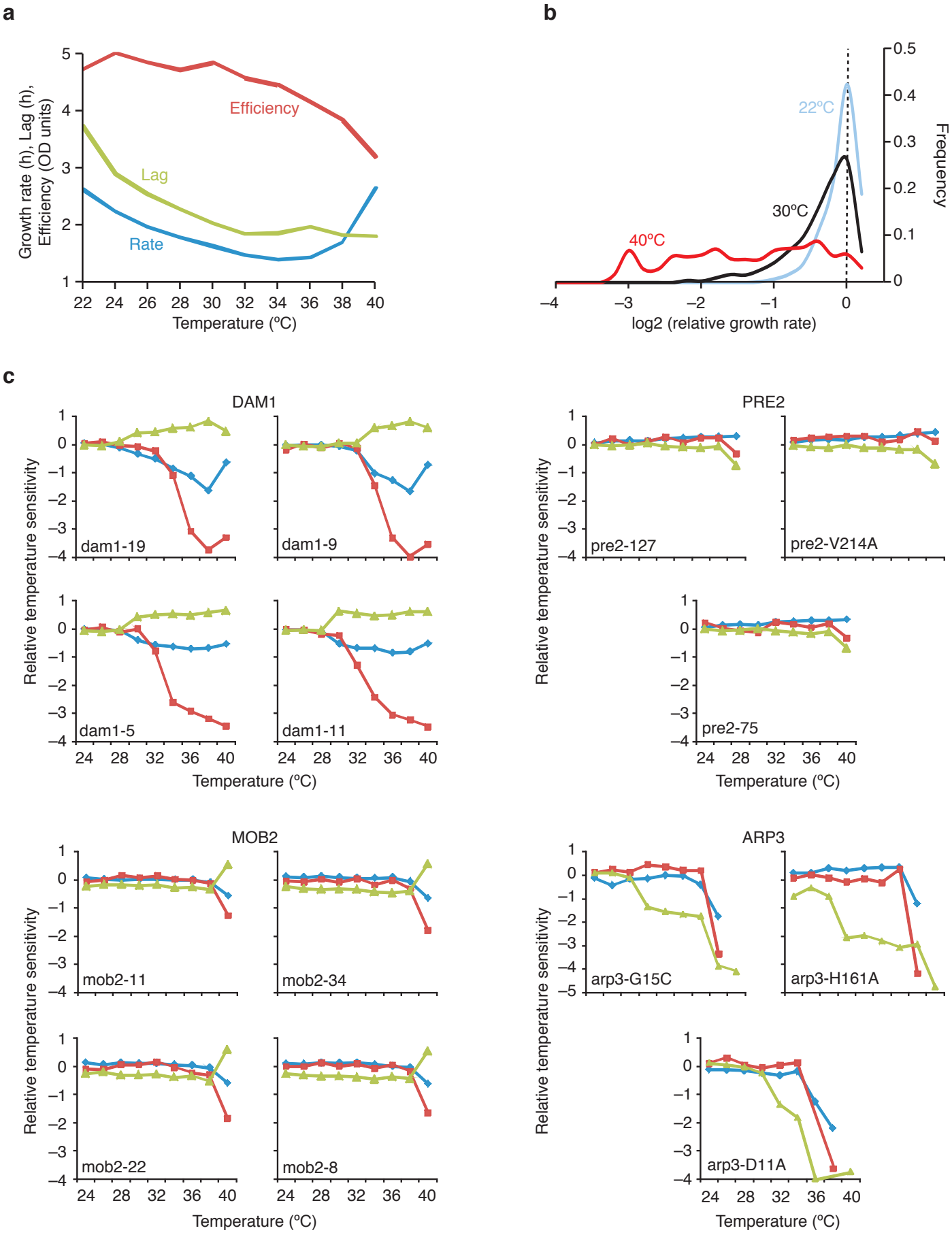

Nature Biotechnology: doi:10.1038/nbt.1832

Supplementary Figure 2 (continued)

d

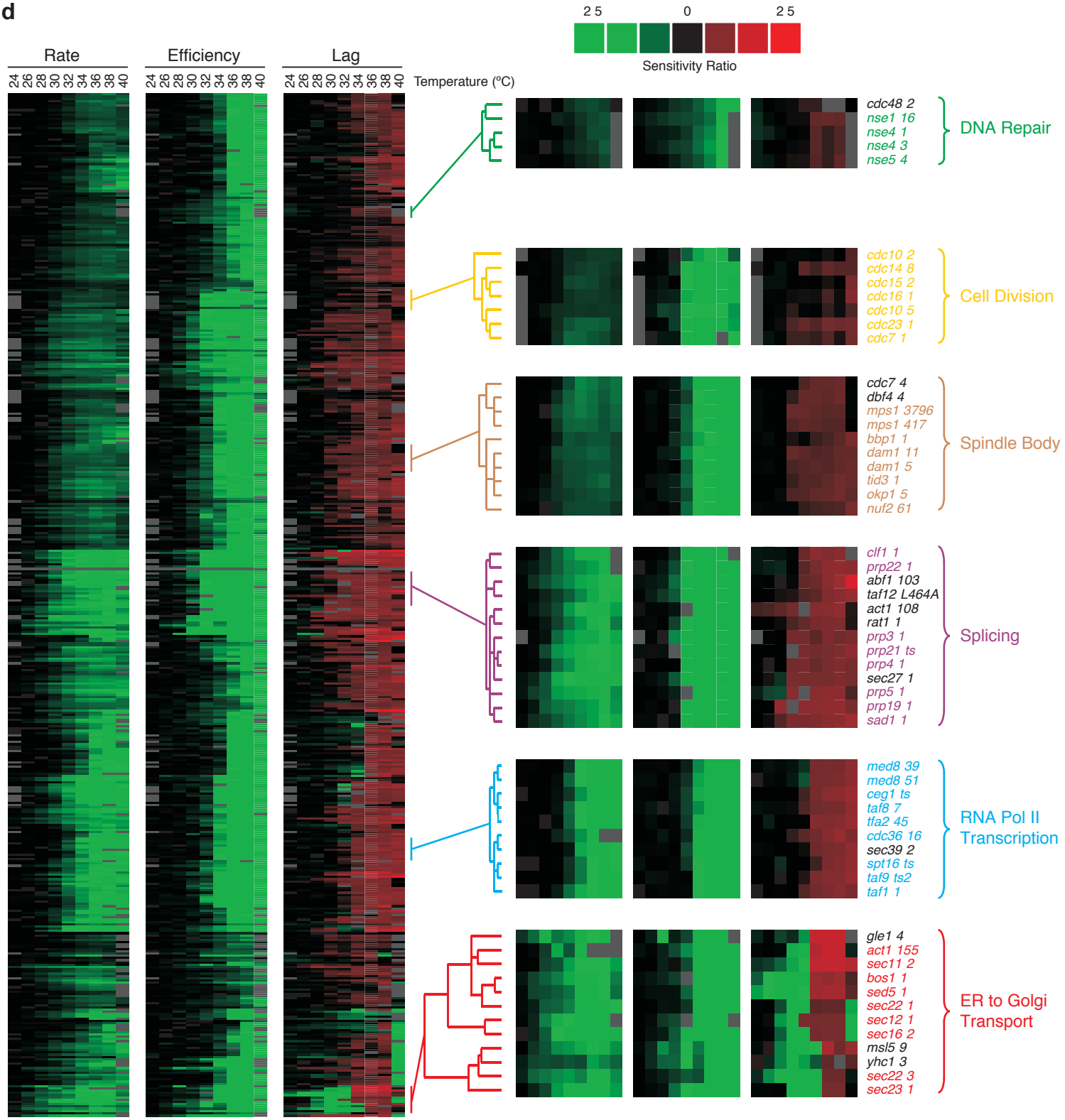

Supplementary Figure 2. Profiling the Temperature Sensitivity of ts Alleles

(a) Liquid growth variables, rate, lag and efficiency of mitotic growth, for the reference WT strain (BY4741, n=72) measured at various temperatures. Growth rate (blue) is given as population doubling time (h), lag (green) is given as time to initiate growth (h), and efficiency (red) is given as the total change in population density (OD units). **(b)** Frequency distribution of the relative growth rate (log2[WT/ts-strain]) for ts alleles at 22°C (blue), 30°C (black) and 40°C (red). Dotted line=0 (WT growth rate). **(c)** Different ts alleles for the same essential genes exhibit similar temperature sensitivity profiles. Growth rate (blue), lag (green) and efficiency (red) were measured at different temperatures for multiple alleles of *DAM1*, *PRE2*, *MOB2* and *ARP3*. **(d)** Uncentered hierarchical clustering of the temperature sensitivity profiles of all ts strains over all temperatures and growth variables using a Pearson similarity metric and average linkage mapping. Functional clusters are indicated and alleles in each cluster are shown in colors.

Nature Biotechnology: doi:10.1038/nbt.1832

Supplementary Figure 3

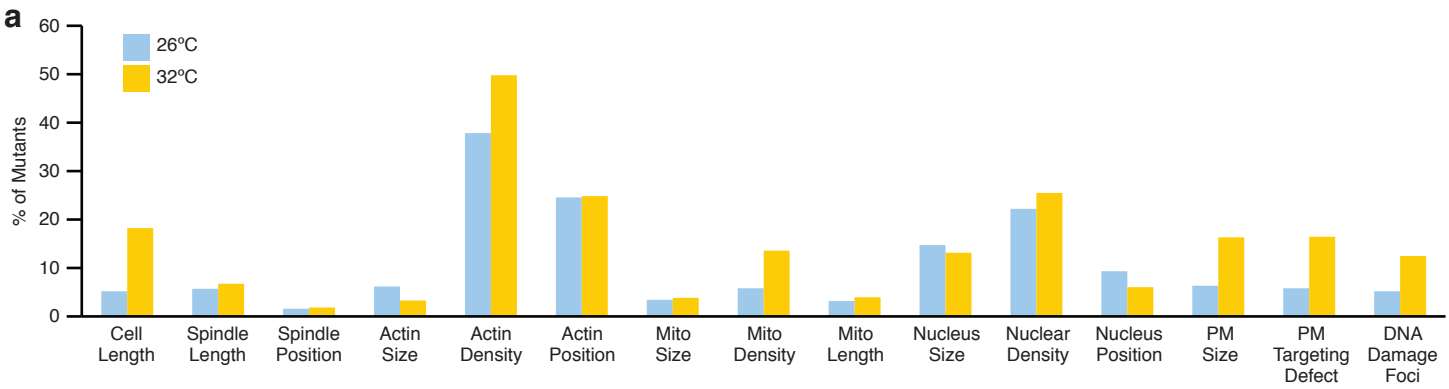

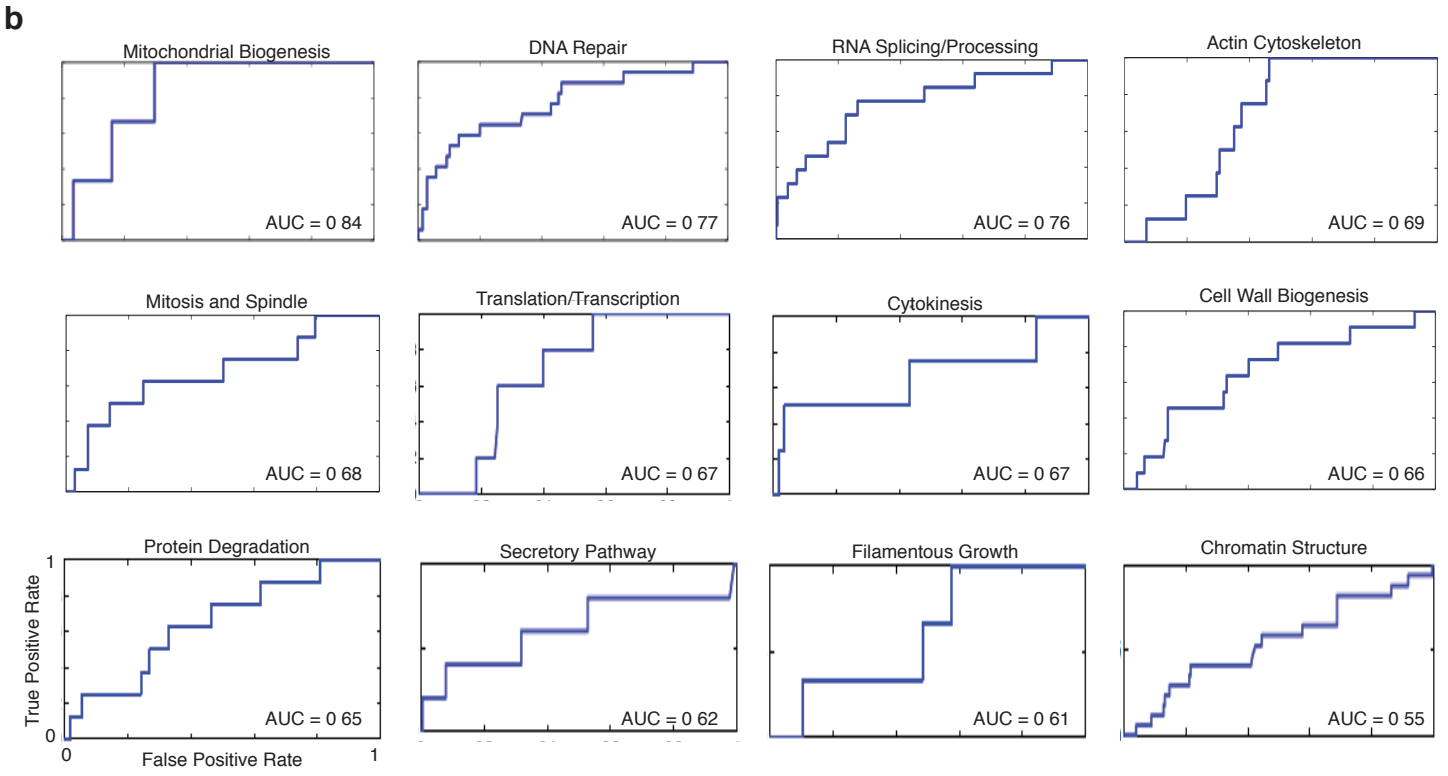

Nature Biotechnology: doi:10.1038/nbt.1832

Supplementary Figure 3

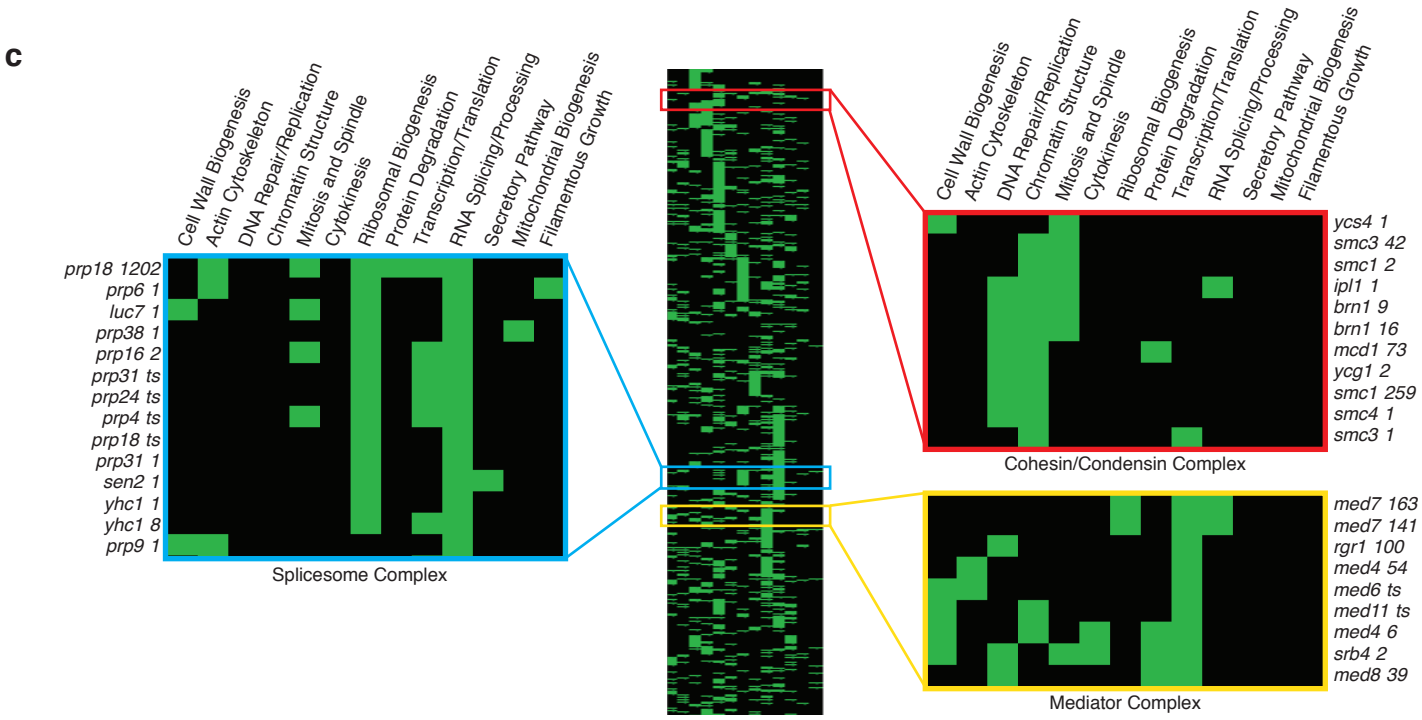

Supplementary Figure 3. Functional Prediction Using HCS Data

(a) Increased temperature exacerbates ts allele phenotypes. The percentage of mutant alleles exhibiting a phenotype that deviated significantly from wild type at both permissive (26°C, blue) and restrictive (32°C, yellow) temperatures was plotted ($P<0.05$, Wilcoxon Rank Sum Test after Bonferroni correction) following normalization. **(b)** Area under the Curve (AUC) scores for functional prediction of different GO categories. Gene functions can be accurately predicted for 12 different functional categories based on HCS data with AUC greater than 0.5. **(c)** Examples of protein complexes predicted to be involved in multiple functions are shown. Genes predicted to be in a given functional category are shown in green. The left and right panels focus on representative gene blocks highlighted in different colors from the global functional prediction matrix.

Nature Biotechnology: doi:10.1038/nbt.1832

Supplementary Figure 4

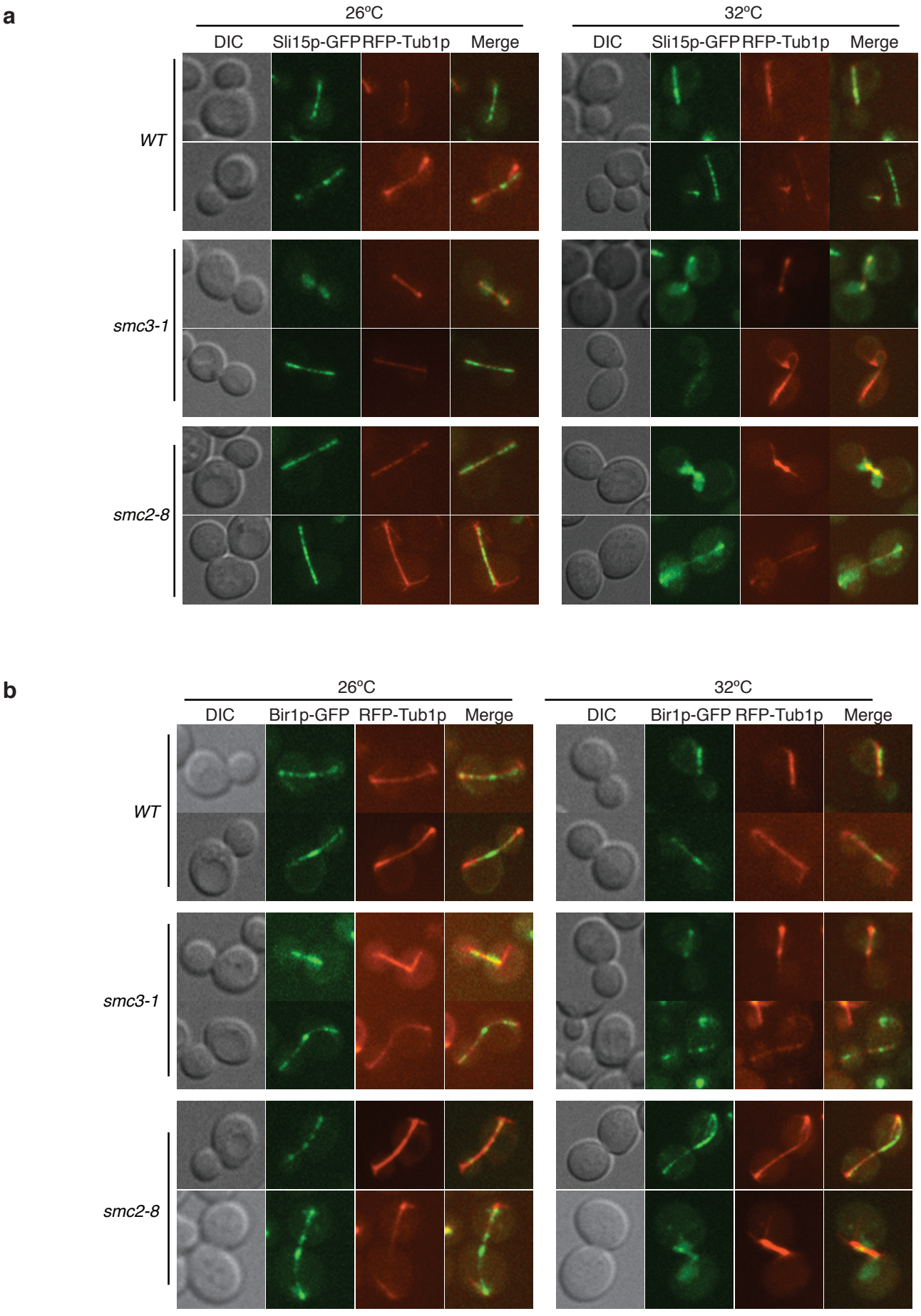

Nature Biotechnology: doi:10.1038/nbt.1832

Supplementary Figure 4 (continued)

c

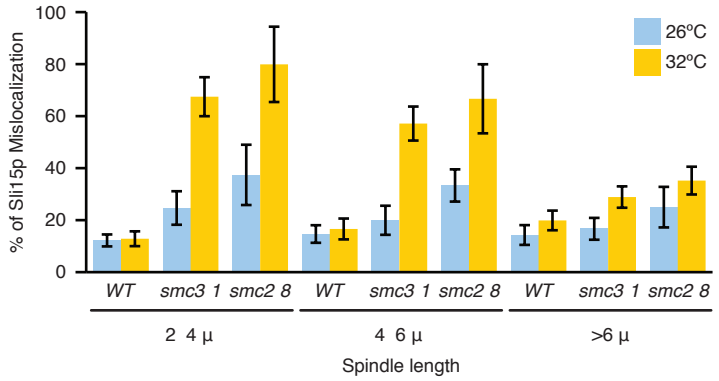

d

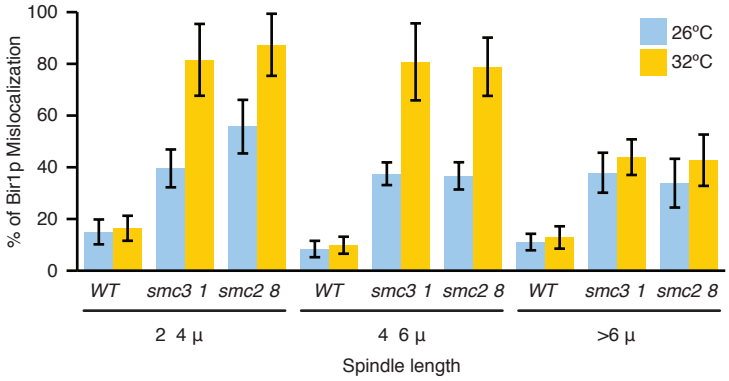

Supplementary Figure 4. Localization of Sli15p-GFP/Bir1p-GFP in Cohesin/Condensin Mutants
(a-b) Subcellular localization of Sli15p-GFP and Bir1p-GFP was monitored using fluorescence microscopy. Cells were grown to mid log phase at permissive temperature (26°C) and then shifted to the restrictive temperature (32°C) for 60 minutes prior to imaging. DIC images, fluorescent micrographs and merged images of representative single cells are shown. **(c-d)** Sli15p-GFP and Bir1p-GFP localization to the mitotic spindle was monitored in wild-type as well as *smc3-1*, and *smc2-8* mutants at permissive (26°C) and restrictive temperatures (32°C). Spindle length was measured in these cells using a RFP-Tub1p marker. Wild-type and mutant cells were divided into three groups based on spindle length (2–4 µ, 4–6 µ, >6 µ). The percentage of cells in each spindle length category that exhibited mis-localized Sli15p-GFP and Bir1p-GFP was measured. Error bars represent the standard deviation across three independent experiments.

Nature Biotechnology: doi:10.1038/nbt.1832

Supplementary Figure 5

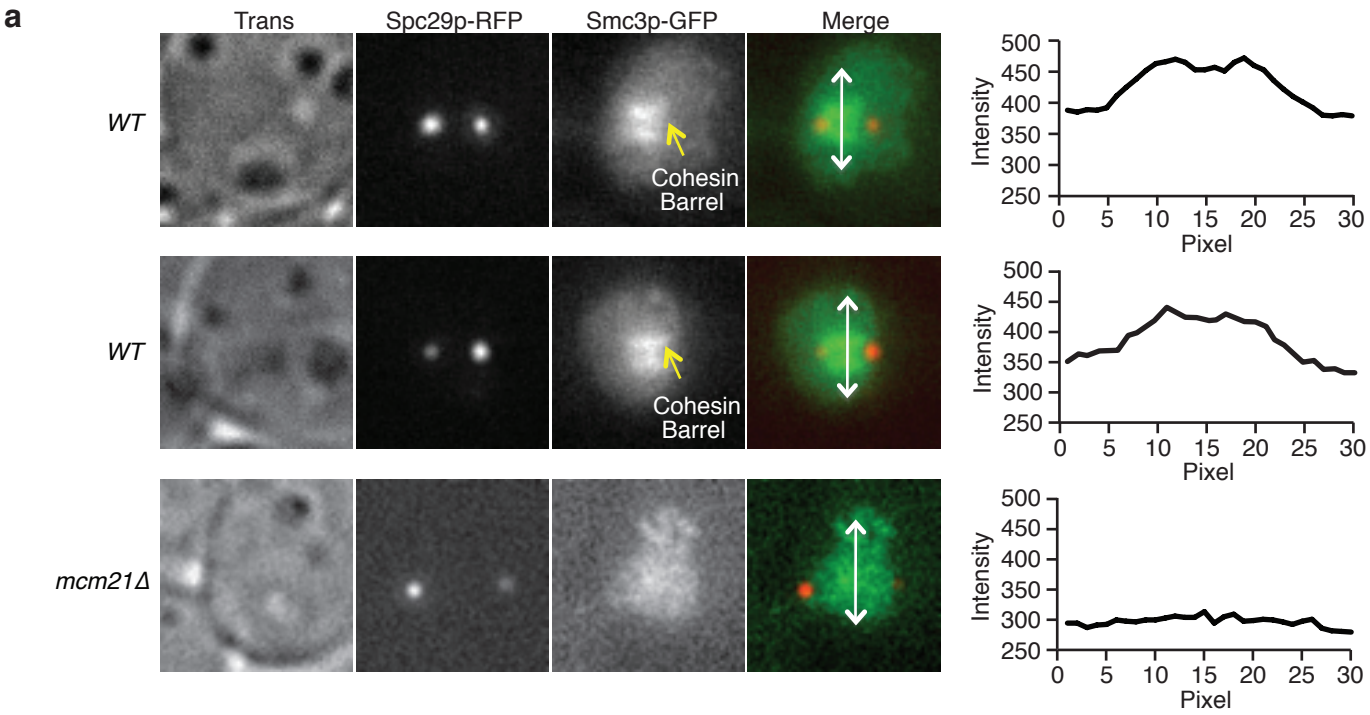

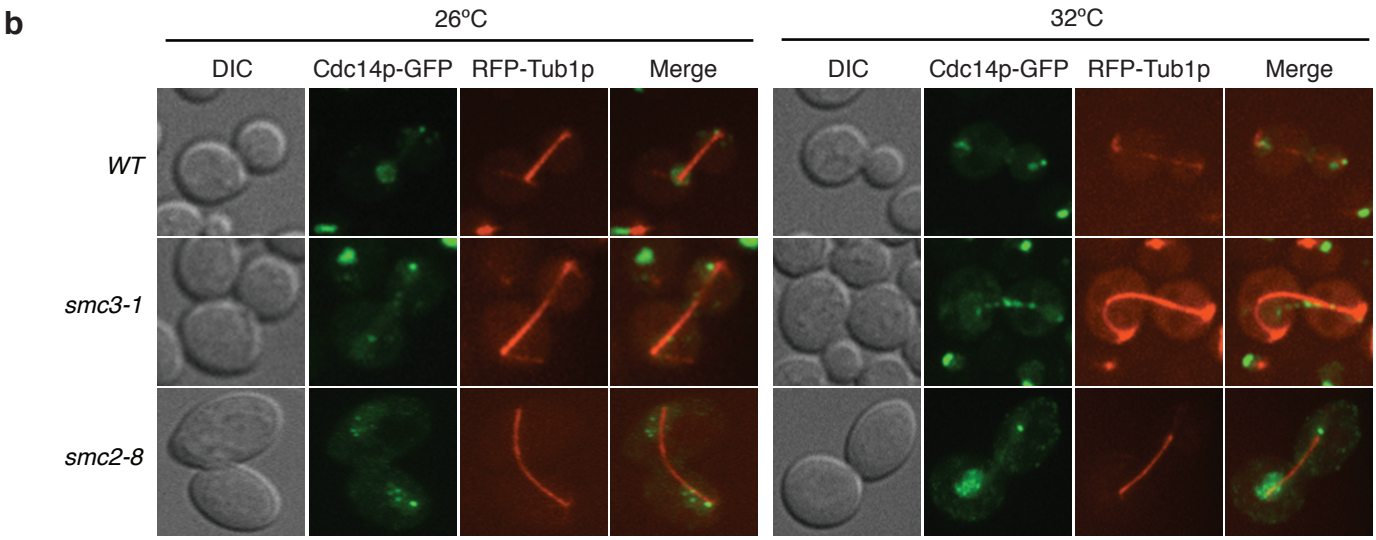

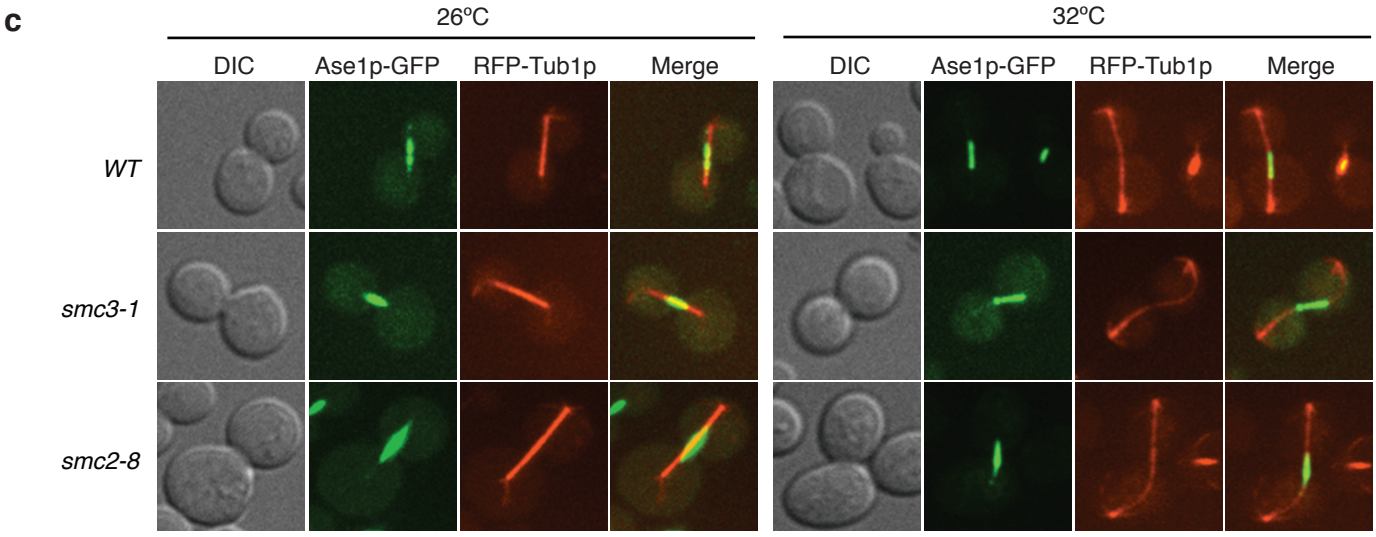

Nature Biotechnology: doi:10.1038/nbt.1832

Supplementary Figure 5 (continued)

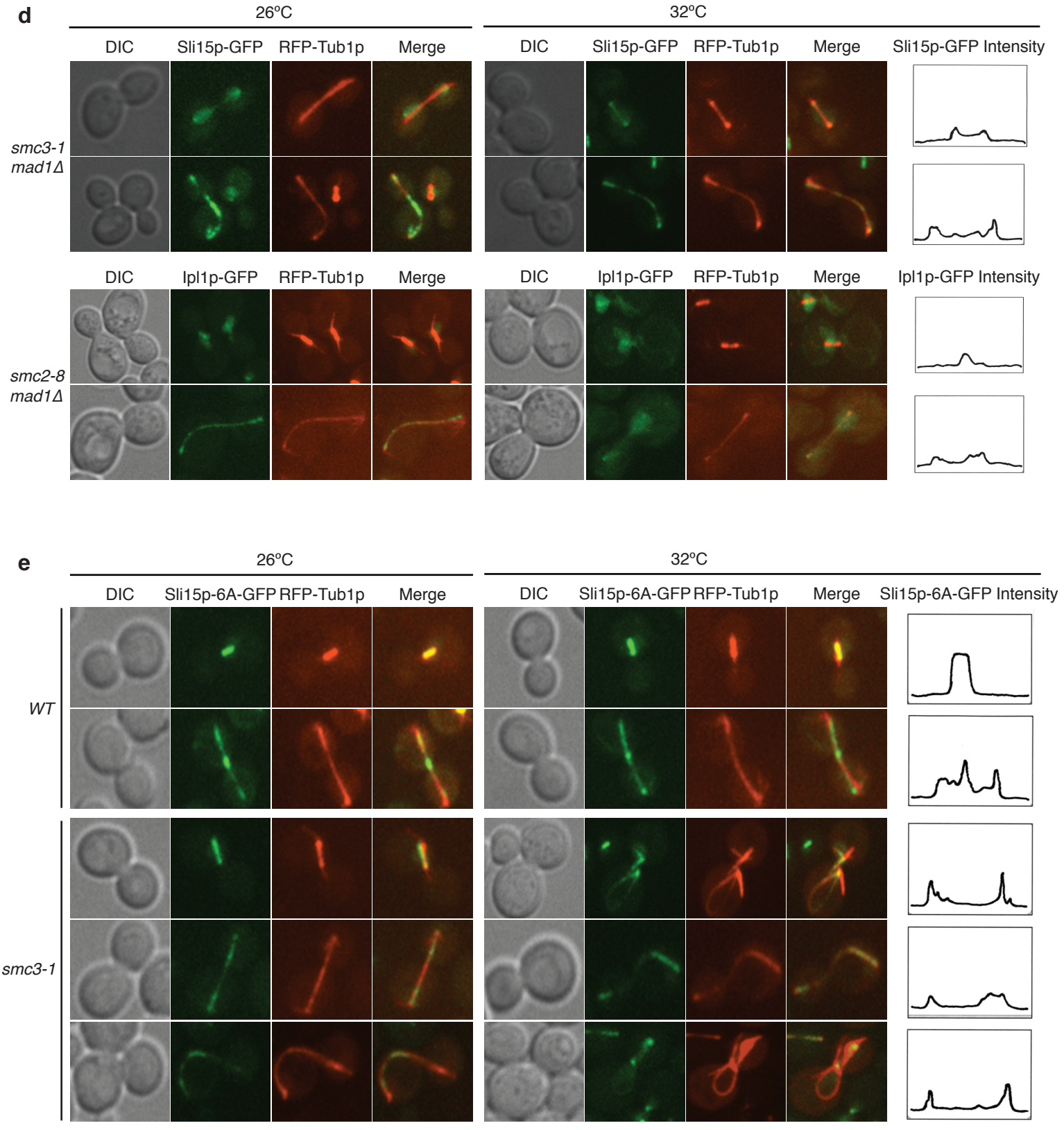

Nature Biotechnology: doi:10.1038/nbt.1832

Supplementary Figure 5 (continued)

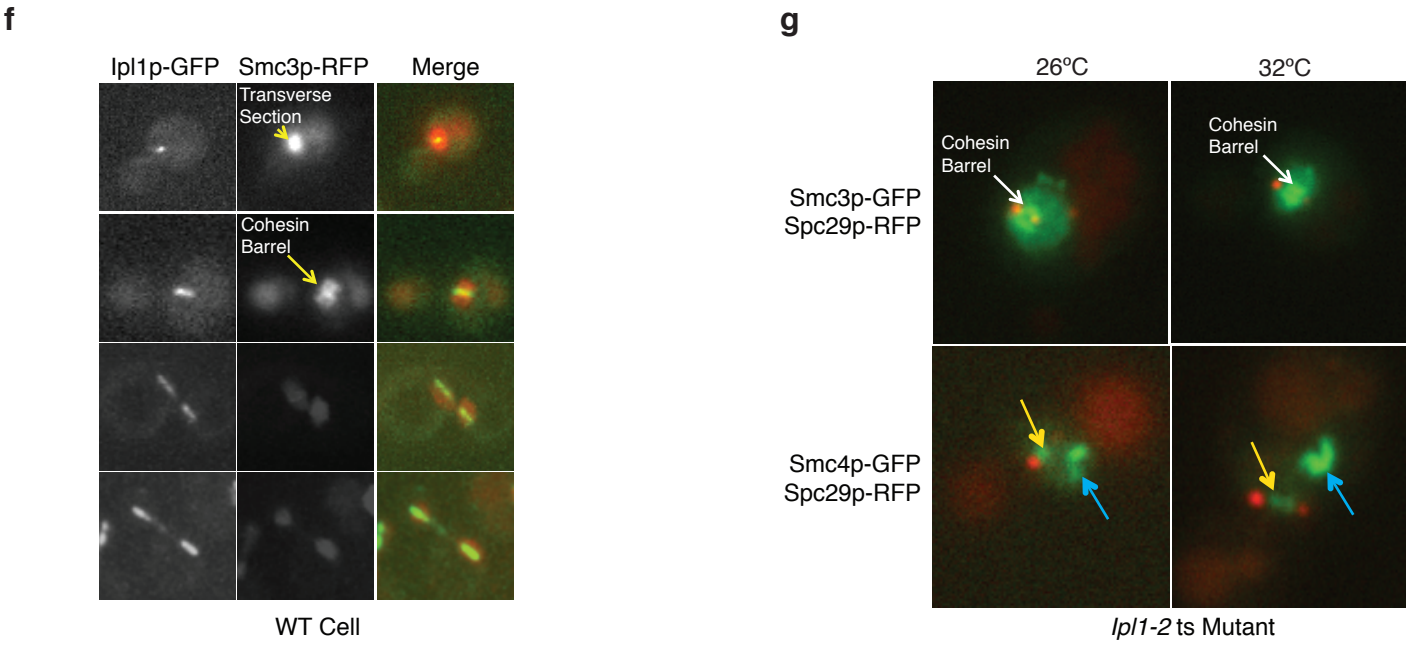

Supplementary Figure 5. Defects in CPC Localization are not Checkpoint Dependent
(a) Cohesin barrel structure was lost in a *mcm21*Δ kinetochore mutant. The top two panels show the distribution of Smc3p-GFP in wild-type cells. The cohesin barrel structure was defined by the two oblongate lobes of fluorescence with an intevening dim region. A representative image of an *mcm21*Δ cell is shown in the bottom panel. The fluorescent intensity line profile across the cohesin barrel is also shown for a representative cell. **(b-c)** Localization of Cdc14p-GFP and Ase1p-GFP in cohesin/condensin mutants. Cells were grown to mid log phase at the permissive temperature (26ºC) and shifted to the restrictive temperature (32ºC) for 60 minutes before imaging. Spindle morphology was monitored using an RFP-Tub1p marker. DIC images, fluorescent micrographs and merged images of representative single cells are shown. **(d)** Localization of Sli15p-GFP and Ipl1p-GFP in *smc3-1 mad1*Δ and *smc2-8 mad1*Δ double mutants. Exponential phase cells were grown at the permissive temperature (26ºC) and shifted to the restrictive temperature (32ºC) for 60 minutes before imaging. Spindle morphology was monitored using an RFP-Tub1 marker. DIC images, fluorescent micrographs and merged images of representative single cells are shown. The fluorescent intensity line profile of Sli15p-GFP and Ipl1p-GFP of a representative cell is also shown. **(e)** Localization of Sli15p-6A-GFP in cohesin mutants. Cells were grown to mid log phase at the permissive temperature (26ºC) and shifted to the restrictive temperature (32ºC) for 60 minutes before imaging. Spindle morphology was monitored using an RFP-Tub1 marker. DIC images, fluorescent micrographs and merged images of representative single cells are shown. The fluorescent intensity line profile of Sli15p-6A-GFP of a representative cell is also shown. **(f)** Localization of Ipl1p-GFP and cohesin (Smc3p-RFP) in wild type cells. Cells were grown to mid log phase before imaging. Fluorescent micrographs and merged images of representative single cells are shown. The top frames represent a budded cell with the transverse section of the mitotic spindle surrounded by the cohesin barrel. **(g)** Co-localization of cohesin/condensin and Spc29-RFP in an *ipl1-2* mutant. Cells were grown to mid log phase at the permissive temperature (26ºC) and shifted to the restrictive temperature (32ºC) for 60 minutes before imaging. Fluorescent micrographs and merged images of representative single cells are shown. Yellow arrows indicate spindle localization and blue arrows indicate rDNA localization.

Supplementary Figure 6

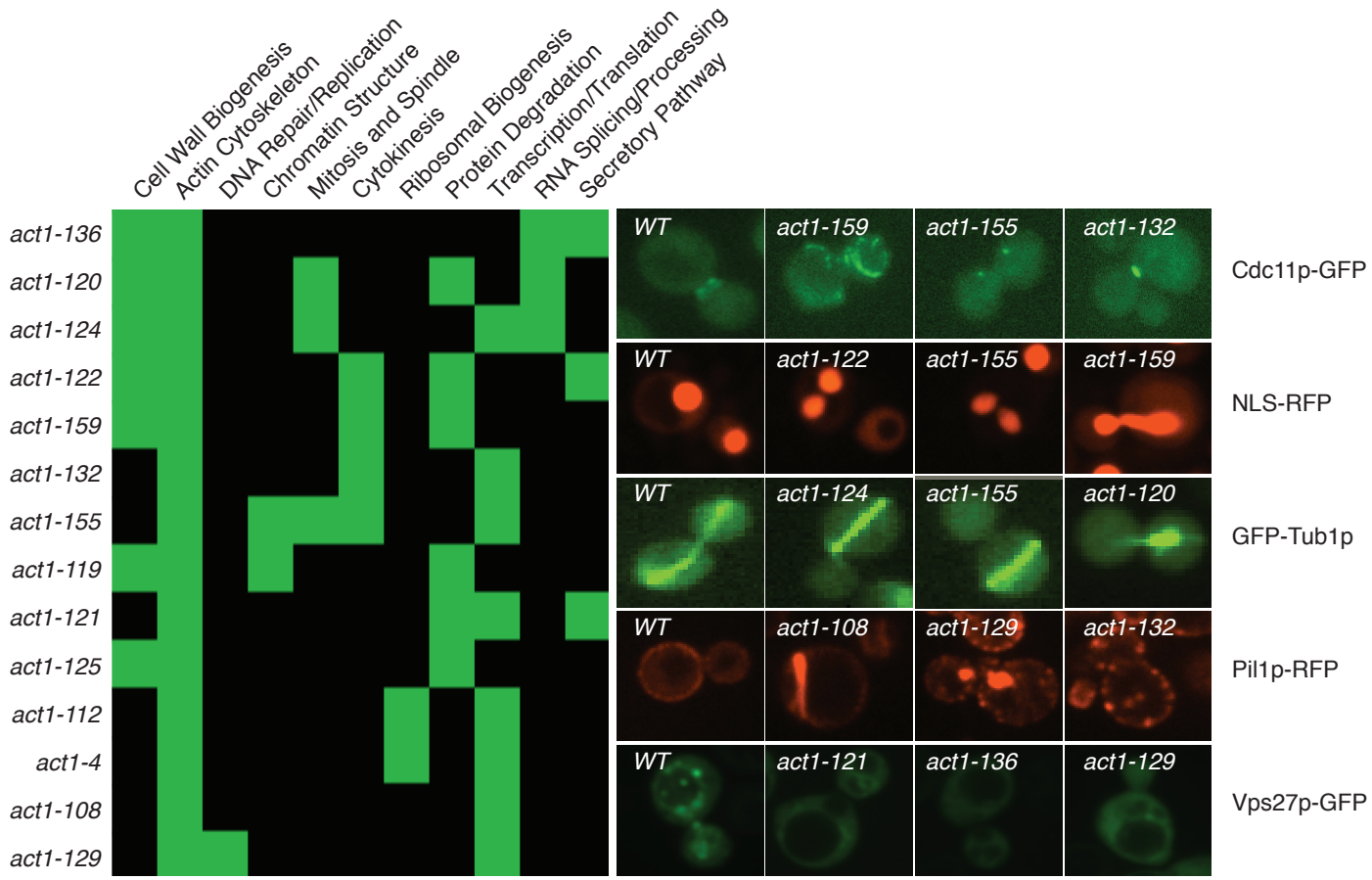

Supplementary Figure 6. Morphological Profiling of Strains Harboring Different *act1* Alleles.
Actin mutant alleles predicted to be involved in multiple functions are shown. Mutant alleles predicted to be in any functional category are labeled in green, others in black. Representative cell images of different mutant cells were evaluated for their role in different biological process at the restrictive temperature using the indicated cellular markers that define different cell compartments.

Nature Biotechnology: doi:10.1038/nbt.1832